Raman Scattering Study of Silicon Carbide Irradiated with 1.25 MeV Si Ions

IOP Conf. Series: Materials Science and Engineering **493** (2019) 012092 doi:10.1088/1757-899X/493/1/012092

Raman Scattering Study of Silicon Carbide Irradiated with 1.25 MeV Si Ions

Pengfei Wang*, Shuai Wang

School of Science, Shandong Jiaotong University, Jinan 250357, People's Republic of China

*Corresponding author. Electronic mail: pfwang0213@126.com

Abstract. Raman spectroscopy was performed to analyze the lattice damage and thermal recovery process of SiC single crystals irradiated by 1.25 MeV Si ions with a fluence of 1.0×10^{16} cm^{-2} at RT, 300°C, and 500°C. The ion irradiation at RT leads to the transformation of SiC from crystalline to amorphous state, which is demonstrated by the appearance of Si-Si, Si-C, and C-C vibration modes. For the irradiation at 300 and 500°C, two of predominant Raman peaks at 1355 and 1578 cm^{-1} are detected. This reveals that the irradiation at elevated temperatures can cause the formation of graphite clusters. The graphite cluster has a poor thermal stability and is removed after annealing at 400°C. The Raman peak at about 576 cm^{-1} appears after the annealing at 800°C. It could originate from $C_{Si}V_C$ defect complex.

1. Introduction

Silicon carbide (SiC) is considered to be promising nuclear material because of its outstanding mechanical performance and radiation resistance. In recent years, investigations of defect structures, recovery mechanism, and irradiation behavior were performed by many groups. The vacancies, interstitials, dislocations, voids, and so on were investigated by means of theoretical calculation and experimental analysis [1-4]. The appearance of irradiation damages brings about the modification in physical and mechanical properties. Therefore, a comprehensive understanding of irradiation damages becomes necessary to applying the SiC in nuclear environment. The simulation of neutron irradiation by using ion irradiation have been implemented widely for several decades. In his paper, we will use ion irradiation technology and analyze the irradiation damage and the influence of irradiation temperature on the production of damages.

2. Experimental

The samples are commercial semi-insulating 6H-SiC single crystals and were purchased from the TankeBlue Semiconductor Co. Ltd, China. The Si ion irradiation was implemented at 320 kV Multi-discipline Research platform for Highly Charged Ions of Institute of Modern Physics, Chinese Academy Sciences. The samples were irradiated by 1.25 MeV Si ions up to the fluence of 1.0×10^{16} cm^{-2} at room temperature (RT), 300°C, and 500°C, respectively. The irradiation profiles were calculated by applying SRIM 2013. In this calculation, the displacement energies of C and Si atoms were selected respectively as 20 and 35 eV. The depth profiles of damage level is exhibited in Fig. 1. The damage levels are about 1 displacements per atom (dpa) near the surface and 5 dpa in the 800 nm zone. The damage levels

gradually increases in the range from sample surface to 800 nm. After the irradiation treatment, the samples were annealed at the temperature ranges from 200°C up to 1000°C in air. All of Raman spectra were obtained by using A Renishaw inVia Raman microscope at RT. The measurement configuration was the backscattering configuration from (0001) sample surface. The excitation wavelength was 532 nm.

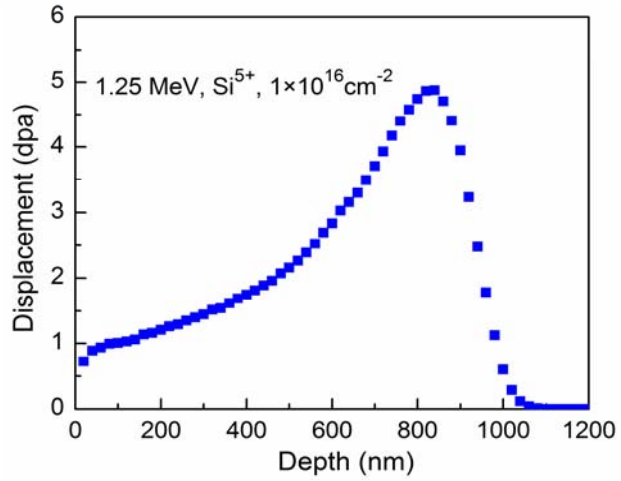

Figure 1. Depth profiles of damage level in Si ion irradiated SiC simulated by SRIM 2013.

3. Results and discussion

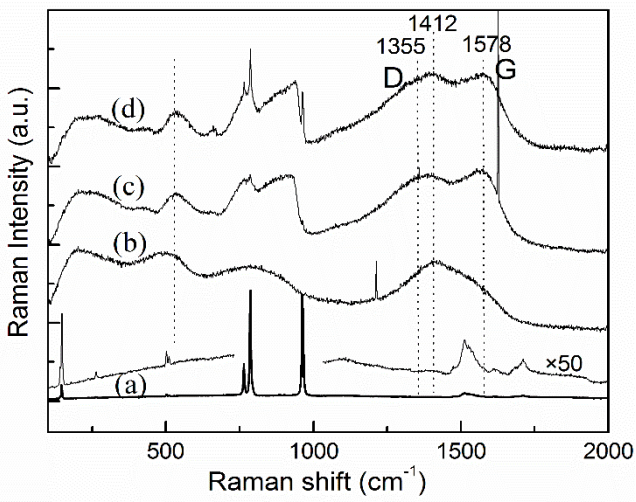

Figure 2. Raman spectra of pristine and as-irradiated SiC. The irradiation temperatures of (a), (b), and (c) are RT, 300 °C, and 500°C, respectively. The irradiation fluence is 1.0×10^{16} cm^{-2}. The Raman spectrum of virgin SiC is magnified 50 times for clear demonstration.

Raman scattering has been widely used for the characterization of materials. The 6H-SiC lattice vibration modes are classified as $6(A_1+B_1+E_1+E_2)$. The A_1 and E_2 modes can be measured in (0001) backscattering configuration. Fig. 2 shows the Raman spectra of the pristine and irradiated SiC. The pristine SiC possesses intrinsic Raman peaks, as shown in Fig. 2 (a). The low-frequency peaks centered at 149, 505, 767, 788, and 966 cm^{-1} arise from first-order Raman scattering, and the high-frequency peaks situated at 1516, 1620, and 1713 cm^{-1} belong to second-order Raman scattering [4, 5]. The ion irradiation can lead to lattice disorder which demonstrated by the change of Raman spectrum. Fig. 2(b)

presents the Raman spectrum of SiC irradiated at RT with a fluence of 1.0×10^{16} cm^{-2}. The above-mentioned Raman peaks disappear completely and three of well-defined Raman peaks at 485, 780, and 1412 cm^{-1} appear. They respectively correspond to the Si-Si, Si-C, and C-C vibration modes and reveal that the irradiation zone was amorphized completely by the Si ion bombardment. More precisely, the peak at 1412 cm^{-1} is ascribed from the sp^2/sp^3 C clusters. In addition, an obscure peak at about 1578 cm^{-1} were also recorded. Irradiation temperature plays an important role in the production of lattice damages. In order to investigate the temperature effect, the Si-ion irradiations at elevated temperatures were also carried out. Fig. 2 (c) presents the Raman spectrum of SiC irradiated at 300°C with a fluence of 1.0×10^{16} cm^{-2}. In low-frequency region, the weak peaks at 425 and 655 cm^{-1} were recorded. They could originate from the Si-Si and Si-C vibrations. The optical phonon peaks located at 767, 788 and 966 cm^{-1} appear and show asymmetric broadening with the tails in the ranges of 704-762 cm^{-1} and 815-927 cm^{-1}, respectively. The asymmetric broadening originates from the phonon confinement effect caused by irradiation defects. It is remarkable fact that two of predominant peaks at 1355 and 1578 cm^{-1}, marked D and G, were detected. They originate from the breathing vibrations of six-member C rings and stretching vibrations of sp^2 C-C bonds [6, 7]. This reveals that the Si ion irradiation at 300°C leaded to the formation of graphite clusters. Fig. 2 (d) presents the Raman spectrum of SiC irradiated at 500°C with a fluence of 1.0×10^{16} cm^{-2}. Comparing to the Raman spectra in Fig. 2 (c), no additional Raman peaks appear and the above-mentioned peaks in Fig. 2 (c) became more distinct. The obvious appearance of intrinsic optical phonon peaks at 767, 788 and 966 cm^{-1} signifies that this irradiation enhanced the dynamic annealing process and resulted in a lower damage level.

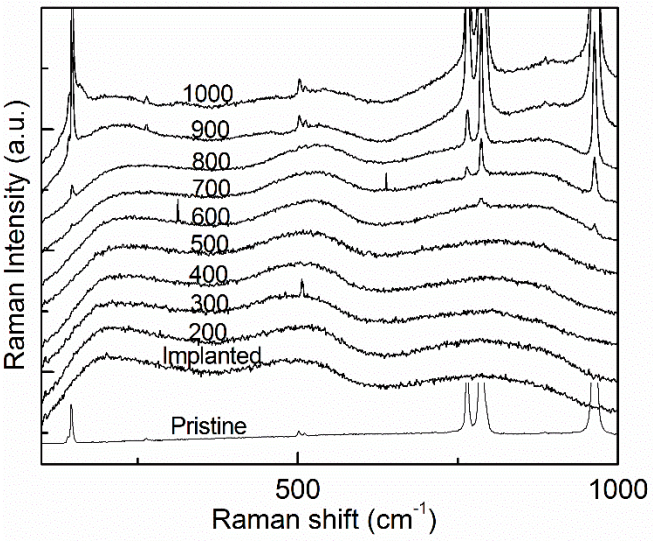

Figure 3. Low-frequency Raman spectra of the SiC irradiated at RT and annealed subsequently at various temperatures.

In some degree, irradiation damages can be removed by thermal treatment. Lattice structure becomes more ordering with the increasing annealing temperatures. After the irradiation, the samples were annealed in the 200-1000°C temperature range. Fig. 3 display the Raman spectra in low-frequency region from the SiC irradiated at RT and subsequently annealed at the temperatures of 200 to 1000°C. The Raman spectra of samples annealed below 500°C remain unchanged. When the temperature increases to 600°C, the optical phonon peaks at 788 and 966 cm^{-1} are detectable and become more obvious with increasing temperature up to 1000°C. The acoustic phonon peaks at149 and 505 cm^{-1} can be measured after 700 and 900 °C annealing, respectively.

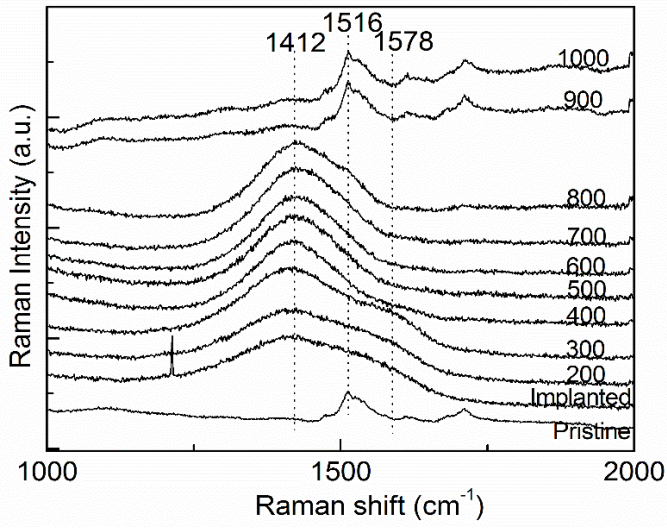

Figure 4. High-frequency Raman spectra of the SiC the SiC irradiated at RT and annealed subsequently at various temperatures.

Fig. 4 shows the Raman spectra in high-frequency region from the SiC irradiated at RT and annealed subsequently at the various temperatures. For the peaks at 1412 cm^{-1}, it can revive during annealing below 800°C and disappear completely after annealing at 900°C. The peaks at 1578 cm^{-1} remains unchanged at 300°C annealing, decreases at 400°C annealing, and disappear completely at 500°C annealing. These reveal that the lattice defects related to the peaks at 1412 and 1578 cm^{-1} have the thermal stability of 800-900°C and 300-400°C. The second scattering peaks at 1516 cm^{-1} can be recorded faintly after the 700°C annealing and becomes obvious after 900°C. These observations indicate the amorphous layer can recrystallize dramatically at 900°C annealing.

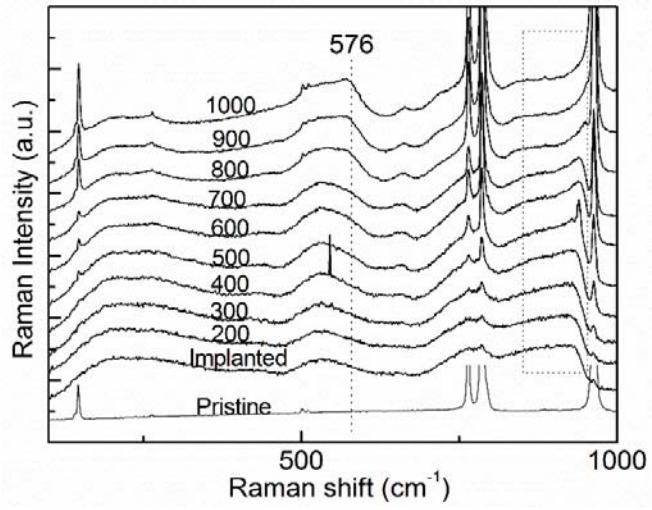

Figure 5. Low-frequency Raman spectra of the SiC irradiated at 300 °C and annealed subsequently at various temperatures.

The irradiation damage and Raman spectrum of the SiC irradiated at 300°C are different from those of SiC irradiated at RT. Hence, the SiC irradiated at 300°C exhibits a different thermal evolution process. Fig. 5 shows the low-frequency Raman spectra of the SiC irradiated at 300°C and annealed subsequently at the temperatures of 200 to 1000°C. The Raman spectra of samples change after every annealing

treatment. The acoustic phonon peak at 149 cm^{-1} and optical phonon peaks at 767, 788, and 966 cm^{-1} are become more and more obvious with increasing temperatures from 200 to 1000°C, but the acoustic phonon peak at 505 cm^{-1} can be measured after 800°C annealing. The asymmetry and tail decreases with the increase of annealing temperature and almost disappear after the annealing at 1000°C. It reveal that the phonon confinement effect is weakened with the recovery of irradiation defects. Furthermore, a Raman peak at about 576 cm^{-1} is detected after the annealing at 800°C and becomes more obvious during the annealing at 900 and 1000°C. For the SiC irradiated at RT, this peak is not recorded during annealing process. The observation reveals that this peak is related to irradiation and the subsequent annealing temperatures. On the basis of its thermal evolution, this Raman peak could originate from $C_{Si}V_C$ defect complex which is transformed from V_{Si} point defect [8].

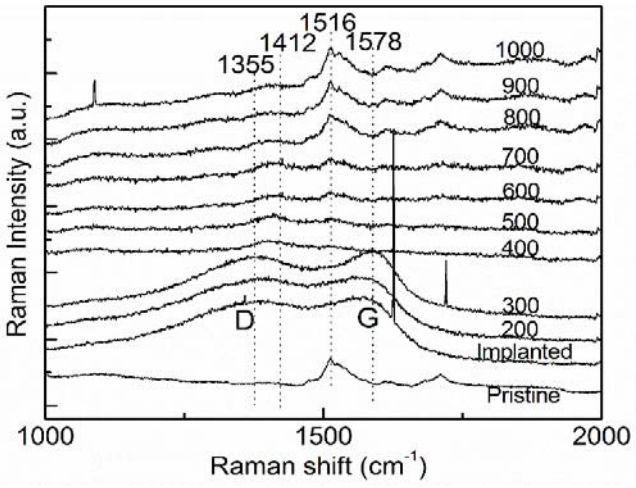

Figure 6. High-frequency Raman spectra of the SiC irradiated at 300°C and annealed subsequently at the various temperatures.

For the irradiation at 300°C, the most interesting fact is that the irradiation leaded to the formation of graphite clusters. This result reveals that the irradiation can cause the precipitation of carbon phase. The stability of graphite clusters is obtained by the thermal annealing. The high-frequency Raman spectra of the SiC irradiated at 300°C and annealed subsequently at the temperatures of 200 to 1000°C are shown in Fig. 6. The D and G peaks remain unchanged after the annealing at 200 and 300°C. When the temperature increases to 400°C, the D and G peaks vanish simultaneously. It is confirmed that the graphite cluster has a poor thermal stability. The peak at 1412 cm^{-1} can keep constant during the annealing at 200-800°C, as shown in Fig. 4. In Fig. 6, the peak at 1412 cm^{-1} is very weak. The observations reveal that the irradiation temperature of 300 can suppress the formation of sp^2/sp^3 C clusters. The second Raman scattering peaks at 1516 cm^{-1} can be recorded faintly after the 500°C annealing and becomes obvious after 800°C. These observations demonstrates that the elevated-temperature irradiation produce relatively lower damage level in comparison with the RT irradiation.

4. Conclusion

To summarize, we investigate the SiC single crystals irradiated by 1.25 MeV Si ions with a fluence of 1.0×10^{16} cm^{-2} at room temperature (RT), 300°C, and 500°C. The ion irradiation at RT can cause the transformation from crystalline to amorphous state. For the irradiation at 300 and 500°C, two of predominant Raman peaks at 1355 and 1578 cm^{-1} demonstrate the formation of graphite clusters. The graphite cluster has a poor thermal stability and is removed after annealing at 400 °C. The Raman peak at 576 cm^{-1} could originate from $C_{Si}V_C$ defect complex.

Acknowledgements
This work was supported by National Natural Science Foundation of China (Grant No. 11505107), Shandong Provincial Natural Science Foundation, China (Grant No. ZR2015AL022), and Doctor Foundation of Shandong Jiaotong University.

References
[1] F. Gao, W.J. Weber, Phys. Rev. B 66 (2002) 024106.
[2] E. Jin, L.S. Niu, Physica B 406 (2011) 601 - 608.
[3] S. Nakashima, T. Mitani, J. Senzaki, H. Okumura, T. Yamamoto, J. Appl. Phys. 97 (2005) 123507.
[4] S. Sorieul, J.-M. Costantini, L. Gosmain, L. Thomé, J.-J. Grob, J. Phys.: Condens Matter 18 (2006) 5235 - 5251.
[5] S. Nakashima, H. Harima, Phys. Stat. Sol. (a) 162 (1997) 39 - 63.
[6] W. Jiang, Y. Zhang, M.H. Engelhard, W.J. Weber, G.J. Exarhos, J. Lian, R.C. Ewing, J. Appl. Phys. 101 (2007) 023524.
[7] F. Tuinstra, J.L. Koenig, J. Chem. Phys. 53 (1970) 1126.
[8] P. F. Wang, L. Huang, W. Zhu, Y.F. Ruan, Solid State Commun. 152 (2012) 887 - 890.